

Adsorption of Direct of Yellow ARLE Dye by Activated Carbon of Shell of Coconut Palm: Diffusional Effects on Kinetics and Equilibrium States

Aparecido Nivaldo Módenes¹, Fabiano Bisinella Scheufele^{1*},
Fernando Rodolfo Espinoza-Quiñones¹,
Patrícia Simões Carraro de Souza¹, Camila Raquel Betin Cripa¹,
Joelmir dos Santos¹, Vilmar Steffen^{1,2}, Alexander Dimitrov Kroumov³

¹Department of Chemical Engineering – Postgraduate Program

West Parana State University

645 Rua da Faculdade, Jardim Santa Maria

85903-000 Toledo, Paraná, Brazil.

E-mails: anmodenes@yahoo.com.br, fabianoscheufele@gmail.com,

f.espinoza@terra.com.br, patricia.carraro@hotmail.com,

camilacripa@gmail.com, joe.dossantos@hotmail.com

²Chemical Engineering Coordination

Federal Technological University of Paraná

Linha Santa Bárbara, w/o No. 85601-971 Francisco Beltrão

Paraná, Brazil.

E-mail: eq.vilmar@hotmail.com

³Department of Applied Microbiology

Division “Microbial Synthesis and Ecology”

Institute of Microbiology “Stephan Angeloff” – Bulgarian Academy of Sciences

Acad. G. Bonchev Str., Bl. 26, Sofia 1113, Bulgaria

E-mail: adkrumov@microbio.bas.bg

*Corresponding author

Received: March 9, 2015

Accepted: June 18, 2015

Published: June 30, 2015

Abstract: In this paper, the characteristics and potential removal of direct yellow ARLE (DYA) dye by using coconut palm shell-based activated carbon (CPS-AC) were assessed. Both kinetic and equilibrium experimental data were obtained from a series of DYA dye sorption experiments. All the sorption experiments were performed in closed batch system under constant temperature and stirring speed, at the predetermined pH of initial solution. The kinetic mathematical models of pseudo-first order, pseudo-second order, Elovich and intra-particle diffusion model were used in order to better interpret the adsorption kinetics phenomenon. Equilibrium data were described by applying the isotherm models of Langmuir, Freundlich, Tóth, Sips and Khan. The best description of DYA sorption equilibrium data was achieved for the Langmuir isotherm model, reaching a maximum adsorption capacity of 100 mg·g⁻¹. Finally, the DYA dye adsorption functional groups characterizations were successfully accomplished and the results elucidated the most important groups linked with CPS-AC surface where molecular interactions could occur. Hence, the quantitative evaluation of equilibrium and kinetic experiments of adsorption process have demonstrated that the CPS-AC adsorbent was a promising high effective adsorbent and its potential can be successfully used for DYA dye removal.

Keywords: Adsorption, Activated carbon characterization, Direct dye removal, Molecular interactions, Surface chemistry, Textural properties.

Introduction

Water pollution is an increasing environmental problem and worldwide concern, which demands immediate complex solution based not only on scientific willingness. Nevertheless, the scientific efforts to solve the environmental problems connected with water pollutants continuously increased. One of the most significant pollutant sources is the textile industry, which consumes large water volumes during the production process and disposes low degradability wastes. This industrial sector generates effluents with several contaminants. The composition of effluents includes acids and caustic solids, toxic compounds and several dyes. Some of these colored compounds are carcinogenic, mutagenic, teratogenic and toxic substances to humans as well as for aquatic species and micro-organisms [2, 37]. Among the used dyes by textile industry, direct ones have considerable importance. Direct dyes are extremely soluble in water, and are mainly used for dyeing cellulose fibers, such as, cotton, viscose, among others [25].

Due to the low degradability of dyes, conventional biologic treatment methods usually have low effectiveness of their removal. Although, there are available many techniques for treatment of this type of effluent such as coagulation [29, 34, 54, 65], electrocoagulation [10, 49, 79], coagulation-flocculation [20, 40, 43, 69], photo-fenton [48, 50, 51], photocatalysis [33, 42, 44, 60, 77], among others. In turn, adsorption processes can be considered as an efficient method because of its ease operation, non-toxicity of the adsorbent and high pollutant uptake levels. Moreover, the possibility of dye recovery and concentration and adsorbent's reuse in the process by cycles of adsorption-desorption, can bring a practical and economic advantage. Key factors affecting the adsorption the process are as follows: nature or chemical and textural structure of the adsorbent, solubility, pH of solution, temperature and molecular diameter of adsorbate [21, 36, 53, 73].

Many adsorbents were used in order to improve the dye removal process from water solution such as soil [64], fungi [6, 74], sawdust [66], clay [15, 22, 59], wheat straw [63, 76, 78, 81], rice straw [12, 13, 23, 28], marine algae [7, 14, 52, 57], sugarcane bagasse [26, 58, 80], banana peel [4, 5, 55], orange peel [5, 17], among others. Activated carbon (AC), nowadays is the most employed adsorbent having a large number of applications at industrial processes. On the contrary of most biosorbents and alternative adsorbents, AC presents high surface areas, including microporous, homogeneous structures, besides chemical, thermal and radiation stability. Hence, on the base of its properties, AC is effectively utilized as adsorbent in large scale at many industrial processes, as well as like catalyst or catalyst support. Its adsorptive properties depend essentially on their grain size, porosity, ash content, carbonization degree and activation method [16, 24, 30, 41, 53, 61, 72].

Therefore, adsorption processes can be considered as challenging treatment method for the removal of wastewater pollutants. It must be noted, that their application depends on the specificity of the system adsorbate-adsorbent, which includes the chemical and textural characteristics of the AC and the chemical and molecular structure of the pollutant.

In this context, the present study aimed to quantitatively investigate of equilibrium and kinetic experiments of adsorption removal process of direct yellow ARLE dye by using AC developed from coconut palm shell as an adsorbent.

Materials and methods

The adsorbent used in this work was a granular activated carbon (CPS-AC) produced from coconut palm shell (oil palm or *Elaeis guineensis*) native from Africa. The CPS-AC is a microporous adsorbent which general and textural specifications are shown in Table 1.

The dye which was used in the adsorption tests was the direct yellow ARLE (DYA) dye (C.I. Direct Yellow 106), with a molecular weight of $1333.10 \text{ g}\cdot\text{mol}^{-1}$ and stoichiometric formula of $\text{C}_{48}\text{H}_{26}\text{N}_8\text{Na}_6\text{O}_{18}\text{S}_6$. A stock solution of $1000 \text{ mg}\cdot\text{L}^{-1}$ was prepared with distilled water and then diluted for adsorption tests as needed. The pH of solutions was adjusted for each test with HCl and NaOH ($0.1 \text{ mol}\cdot\text{L}^{-1}$). Initially, the maximum absorbance wavelength of the DYA dye was determined by using a Shimadzu UV/Visible-1800 spectrophotometer. Molecular absorption spectrophotometric measurements were performed in the spectral range between 350-800 nm, where maximum absorbance was observed at the 404 nm wavelength. A calibration curve was made by using the following concentrations values of DYA dye synthetic solution (1, 5, 10, 15, 20, 25, 30, 35, 40, 50, 60, 75 and $100 \text{ mg}\cdot\text{L}^{-1}$).

Table 1. CPS-AC specifications

General properties	Activation temperature ($^{\circ}\text{C}$)	1200
	Iodine number ($\text{mg}\cdot\text{g}^{-1}$)	885
	Density ($\text{g}\cdot\text{cm}^{-3}$)	0.57
	Moisture (%)	8.5
	Average diameter (mm)	0.63
Textural properties	Specific surface area – S_{BET} ($\text{m}^2\cdot\text{g}^{-1}$)	575
	Micropore surface area – S_{micro} ($\text{m}^2\cdot\text{g}^{-1}$)	416
	Total pore volume – V_{pores} ($\text{cm}^3\cdot\text{g}^{-1}$)	0.34
	Micropore volume – V_{micro} ($\text{cm}^3\cdot\text{g}^{-1}$)	0.32
	Mesopore volume – V_{meso} ($\text{cm}^3\cdot\text{g}^{-1}$)	0.02
	Pore diameter – D_p (nm)	1.2

Adsorbent and dye functional groups characterization

In order to identify the functional groups present both at the CPS-AC surface and at the DYA dye molecule, the samples were analyzed by using a Fourier transform infrared spectroscopy (FTIR) in step by step analysis procedure: (a) DYA dye, (b) activated carbon (CPS-AC) before and (c) after adsorption (CPS-ACA). The FTIR spectra were obtained at mid-infrared region ($4000\text{-}450 \text{ cm}^{-1}$) with 64 accumulations (Perkin Elmer – Frontier). In addition to FTIR analysis, the DYA dye structure was assessed by simulating its molecular geometry by using JSmol (3D render engine) and applying the MMFF94 energy minimization method [27] coded in MolView v2.3.3 software.

Preliminary adsorption tests

Preliminary tests of adsorption process were performed in order to obtain the influence of operational parameters values (particle size, pH and stirring speed) on the uptake of the DYA dye. Each experiment (in batch mode) was performed in triplicate by using Erlenmeyers flasks of 125 mL containing 50 mL of synthetic dye solution and adding 0.3 g of adsorbent. After the sorption experiments, samples were centrifuged by 5 minutes at 3000 rpm in order to separate the CPS-AC adsorbent from the solution. The dye concentrations in the samples were determined by UV-Vis spectrophotometer.

In the granulometry tests, the whole amount of CPS-AC adsorbent was separated in three particle sizes by using the sieves of 28 (0.589 mm), 35 (0.500 mm) and 80 mesh (0.177 mm), respectively. The granulometry experiments were performed for all three granulometric sizes, and as well as for CPS-AC adsorbent without granulometric separation. For each test, 50 mL solution with initial value of $\text{pH} = 2$ containing $70 \text{ mg}\cdot\text{L}^{-1}$ of DYA dye were added to 0.3 g of adsorbent. Further, the samples were placed in orbital shaker for 48 hours under controlled stirring speed (90 rpm) and temperature ($30 \text{ }^\circ\text{C}$). After each dye adsorption experiment, CPS-AC adsorbent was separated by centrifugation under 3000 rpm during 5 minutes. The liquid phase of the samples was analyzed by UV-Vis spectrophotometer and the dye concentrations were determined.

The influence of initial pH value on dye removal process was evaluated by changing solution's initial pH in the range from 2 up to 12. For each test, 50 mL solution containing $70 \text{ mg}\cdot\text{L}^{-1}$ of DYA dye was added to 0.3 g of adsorbent (0.177 mm). Then samples were kept for 48 hours under controlled stirring speed (90 rpm) and temperature ($30 \text{ }^\circ\text{C}$) at orbital shaker. After each dye adsorption experiment, CPS-AC adsorbent was separated by centrifugation as mentioned above, and further the liquid phase of the samples was analyzed by UV-Vis spectrophotometer and the dye concentrations were determined.

Finally, experiments were performed under three different stirring speeds (60, 90 and 120 rpm) and similar procedure for samples preparing was used as follows. For each test, 50 mL solution at the initial $\text{pH} = 2$ containing $70 \text{ mg}\cdot\text{L}^{-1}$ of dye was added to 0.3 g of adsorbent (0.177 mm). Samples were transferred to an orbital shaker and the duration of adsorption process was 48 hours at constant temperature ($30 \text{ }^\circ\text{C}$). The CPS-AC separation procedure and the DYA dye concentration measurements were performed as described above.

Adsorption kinetics

The adsorption kinetic tests (in batch system) were performed in triplicate by using Erlenmeyers flasks of 125 mL containing 50 mL of synthetic dye solution and 0.3 g of adsorbent. The parameters values were as follows: initial pH (2.0), adsorbent particle size (0.177 mm) and stirring speed (120 rpm). These working conditions were considered best during the preliminary tests. All samples were kept under controlled stirring speed and temperature ($30 \text{ }^\circ\text{C}$) and withdrawn at different pre-determined times. After the adsorption experiment, separation of solid phase was performed by centrifugation under 3000 rpm during 5 minutes. The DYA dye concentration of the liquid phase of the each sample was determined by UV-Vis spectrophotometer. The dye uptake was calculated by using the mass balance equation presented by Eq. (1).

$$q(t) = \frac{V(C_0 - C(t))}{m_s}, \quad (1)$$

where $q(t)$ is the amount of adsorbed dye per mass of adsorbent at a given time t ($\text{mg}\cdot\text{L}^{-1}$); V is the solution volume (L); C_0 is the initial dye concentration of solution ($\text{mg}\cdot\text{L}^{-1}$); $C(t)$ is the dye concentration of solution at a given time t ($\text{mg}\cdot\text{L}^{-1}$); t is the time of the experiment (h) and m_s is the dry adsorbent mass (g).

Adsorption equilibrium tests

The adsorption equilibrium tests (in batch system) were performed in triplicate by using Erlenmeyers flasks of 125 mL containing 50 mL of synthetic dye solution with different concentrations (from 20 to 500 mg·L⁻¹) and 0.3 g of adsorbent. The samples were placed in orbital shaker and the chosen time was sufficient in order to reach the equilibrium state under the following conditions: initial pH = 2.0 of the solution; adsorbent particle size of 0.177 mm; and stirring speed of 120 rpm. After the adsorption equilibrium experiment, separation of solid phase was performed by centrifugation under 3000 rpm during 5 minutes. The dye concentration of the liquid phase of the each sample was determined by UV-Vis spectrophotometer. The dye uptake at equilibrium state was calculated according to the mass balance expressed by Eq. (2).

$$q_{eq} = \frac{V(C_0 - C_{eq})}{m_s}, \quad (2)$$

where C_{eq} is the dye solution concentration at equilibrium (mg·L⁻¹); q_{eq} is the amount of adsorbed dye per mass of adsorbent at equilibrium (mg·g⁻¹).

Adsorption isotherms

The well-known adsorption isotherms are models, which evaluated parameters values represent the equilibrium phenomenon of a substance uptake from a fluid medium to a solid phase, under fixed working conditions (pH and temperature) [3, 45]. Experimental data of DYA dye adsorption onto CPS-AC were fitted by applying five isotherm models presented in Table 2. The models represent different hypothesis of adsorption process.

Table 2. Adsorption isotherms

Isotherm	Equation	Features	Reference
Langmuir	$q_{eq} = \frac{q_{max} b C_{eq}}{1 + b C_{eq}}$	Monolayer adsorption on homogeneous surface	Langmuir [39]
Freundlich	$q_{eq} = k (C_{eq})^n$	Empiric model applicable to multilayer adsorption on heterogeneous surface	Freundlich [19]
Tóth	$q_{eq} = \frac{q_{max} b_T C_{eq}}{\left(1 + (b_T C_{eq})^{n_T}\right)^{\frac{1}{n_T}}}$	Multilayer adsorption on homogeneous surface	Tóth [71]
Sips	$q_{eq} = \frac{q_{max} b_S C_{eq}^n}{1 + b_S C_{eq}^n}$	Multilayer adsorption on homogeneous surface	Sips [67]
Khan	$q_e = \frac{q_{max} b_K C_{eq}}{(1 + b_K C_{eq})^{n_K}}$	Multilayer adsorption on homogeneous surface	Khan, Ataullah [32]

Adsorption kinetics models

The adsorption kinetics models describe the dynamics of mass transfer between fluid and solid phases. The most common used kinetic models were applied to fit the data of DYA dye adsorption onto CPS-AC and they are presented in Table 3.

The mass transfer resistance due to intra-particle diffusion can exert influence on adsorption process. This phenomenon can be studied by applying the model proposed by Weber and Morris [75], where the constant (C) is related to the boundary layer diffusion and its value is evaluated by linear coefficient one. When the intra-particle diffusion is the only limiting step of the adsorption process, the intercept value is equivalent to zero, and the linear fit pass through the origin. However, three distinct regions are commonly found in the graph of kinetic model of intra-particle diffusion, indicating that there is more than one significant diffusion stage in the process (i.e. external, macro-pores and/or micro-pores diffusion).

Table 3. Adsorption kinetics models

Model	Equation	Features	Reference
Pseudo-first order	$\frac{dq(t)}{dt} = k_1 (q_{eq} - q(t))$	Based on adsorbent uptake capacity	Lagergren [38]
Pseudo-second order	$\frac{dq(t)}{dt} = k_2 (q_{eq} - q(t))^2$	Adsorption/desorption rate controls the process	Blanchard, Maunaye [8]
Elovich	$\frac{dq(t)}{dt} = \alpha \exp(-\beta q(t))$	Involves chemical adsorption process. For adsorbents with heterogeneous surface	Low [46]
Intra-particle diffusion	$q(t) = k_{dif} \sqrt{t} + C$	Intra-particle diffusion resistance influences the adsorption process	Weber and Morris [75]

Optimal values of models parameters (kinetics, diffusion and equilibrium) were obtained by nonlinear identification procedure by using Origin[®] 8.0 Pro software, with *Asymptotic-Symmetry based* method, where the objective function F_{obj} was based on least square statistical criterion (see Eq. (3)).

$$F_{obj} = \sum (q_{exp} - q_{pred})^2, \tag{3}$$

where q_{exp} and q_{pred} are amount of dye adsorbed at equilibrium determined experimentally and predicted by the isotherm model, respectively ($\text{mg} \cdot \text{g}^{-1}$).

Results and discussion

Adsorbent and DYA dye functional groups characterization

The FTIR spectrum of DYA dye (see Fig. 1a) shows that the band at 3460 cm^{-1} can be attributed to the N–H stretching. At 2923, 1639, 1455, 1059 and 618 cm^{-1} one can see typical vinyl groups (C=C) vibrations present at aromatic rings, which can be constituents of vinyl sulfone reactive group of the dye. In addition, a small band at 2854 cm^{-1} can be related to C–H stretching. At 1590 cm^{-1} the N=N stretching characterizes the DYA as an azo dye. The band at 1480 and 1385 cm^{-1} most likely can be linked to N–H and C–H bending vibrations, respectively. Further, at 1354 cm^{-1} a band from S–O stretching, two strong bands at 1183 and 1127 cm^{-1} and a smaller one at 1078 cm^{-1} , which are all vibrations from sulfonate groups ($-\text{SO}_3^-$) and also at 618 cm^{-1} from C–S stretching, indicate the presence of the reactive vinyl sulfone groups ($\text{R}-\text{HC}=\text{CH}-\text{SO}_3^-$). At 1025 cm^{-1} a band is assigned to C–N stretching. In the region from 1000 up to 600 cm^{-1} , small intensity bands are related to out-of-plane

bending vibrations from aromatic structures. Finally, at 547 cm^{-1} another band is associated to the sulfonate groups [9, 56, 68].

In summary, the infrared bands encountered to DYA dye confirm the molecular structure ($\text{C}_{48}\text{H}_{26}\text{N}_8\text{Na}_6\text{O}_{18}\text{S}_6$), where bond vibrations were found and they related to aromatic rings, nitrogen groups (e.g. azo compound), as well as vinyl sulfone and sulfonate groups. They most likely can be the reactive groups and also to give anionic character of this dye [35].

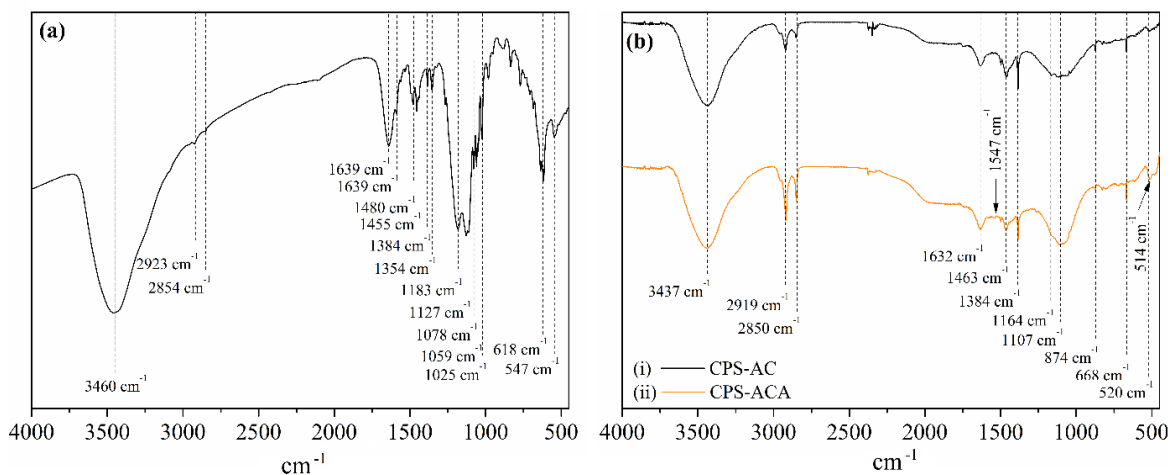


Fig. 1 FTIR analysis: (a) DYA dye; (b) CPS-AC and CPS-ACA.

In order to evaluate the molecular structure and dimensions of DYA dye, a molecular mechanics force fields (MMFF94) simulation was performed, based on the energy minimization (see Fig. 2). By analyzing the functional groups identified by the IR analysis of the DYA dye one may recognize sulfonate; azo; nitrogen and carbonic rings. According to the energy minimization method, the approximate 3D geometry of DYA dye molecular structure can be evaluated as follows: longitudinal diameter is 4.0 nm and the latitudinal diameters of the front and side view is 1.1 and 0.8 nm, respectively.

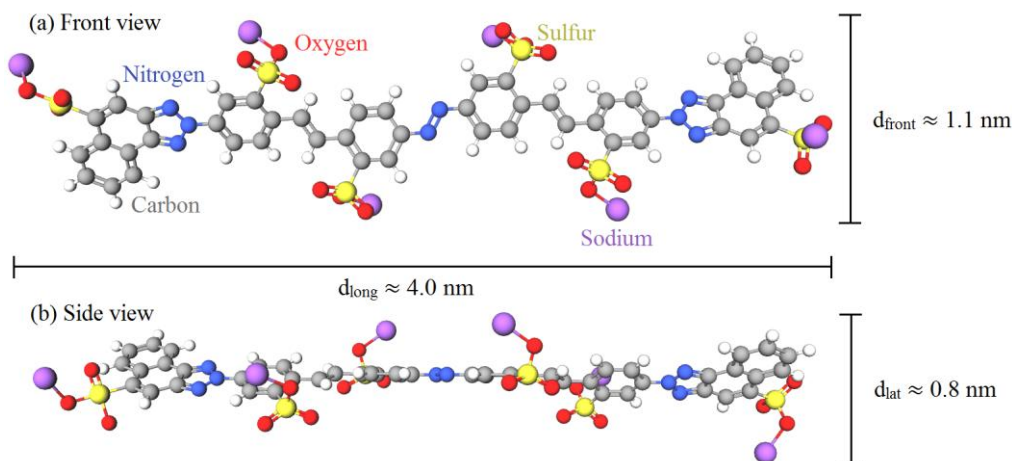


Fig. 2 Molecular structure of DYA dye: (a) front view; (b) side view.

Moreover, considering the DYA dye composition, 24 H-bond acceptors (A) takes place in its structure as shown in Fig. 3. In addition, the six sulfonic groups observed by using IR analysis remain in anionic form ($-\text{SO}_3^-$) in solution under acidic pH, making therefore the DYA dye an anionic one [15].

In addition, the IR spectra of activated carbon before and after the adsorption process are shown in Fig. 1b. Firstly, analyzing the CPS-AC spectrum (i) one can see a large band at 3437 cm^{-1} corresponding to characteristic stretching vibrations of O–H and N–H [1]. Two bands at 2919 and 2850 cm^{-1} are related to C–H symmetrical and asymmetrical stretching. The bands at 1632 , 1463 and 1384 cm^{-1} can be associated to asymmetrical and symmetrical stretching vibrations of C–O bond, present in carboxylic groups [11, 56]. At 1164 cm^{-1} the asymmetrical deformation from C–O–C are derived from cellulosic structure of the precursor material of the AC [11, 51]. The broad overlapping band in the region between 1150 up to 1000 can be also ascribed to C–O vibrations, which can be found in ether, ester, phenolic and carboxylic groups [47, 62]. In the region from 900 up to 600 cm^{-1} two small bands (874 and 668 cm^{-1}) associated to out-of-plane deformation of C–H from aromatic structures [70]. Finally, the 520 cm^{-1} band can be related to phenyl ring torsion [56].

By comparing the CPS-AC and CPS-ACA spectra some slight differences were observed at the bands position and intensities, which were confirmed by the low correlation value ($r^2 = 0.8413$). The bands at 1632 and 1384 cm^{-1} characteristic from the carboxylic groups showed a small increase of the area after adsorption process. Furthermore, a more significant change in both intensity and shape was observed at the broad band from 1150 up to 1000 also related to C–O vibrations, which can be attributed to phenolic and carboxylic groups. Therefore, the CPS-ACA results clearly pointed out that the carboxylic groups were the main sites responsible to DYA dye adsorption.

Carboxylic groups can frequently act as adsorption sites, due to its reactivity, where strong electrostatic interactions may appear, where the pH of the solutions favors the dye sorption process. For anionic DYA dye (see Fig. 3), electrostatic interactions between positively charged carboxylic ($-\text{COOH}_2^+$) and sulfonate groups ($-\text{SO}_3^-$) most likely could be responsible for the adsorption process. Moreover, H-bonds can be formed between carboxylic and phenolic groups present at the CPS-AC surface and nitrogenated and oxygenated groups taking place in the dye molecule (H-bond acceptors, see Fig. 3).

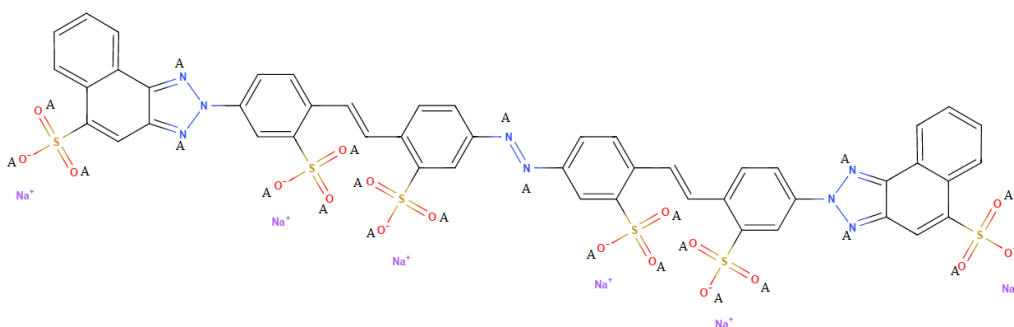


Fig. 3 Structural formula of DYA dye

Additionally, the increased band at 1107 cm^{-1} may be a shifted band associated to the S–O stretching in the dye structure, as previously seen at the 1127 cm^{-1} during the DYA dye IR analysis. Another difference between the spectra was the appearing of the small band at 1547 cm^{-1} due to the C=C stretching vibration, which can be attributed to the aromatic rings in the dye structure. Finally, the phenyl ring torsion band at 520 cm^{-1} shifted to 514 cm^{-1} , this modification most probably indicate that the sorption process may be also driven by van der Waals (hydrophobic interactions) besides the electrostatic interactions, although their intensity are much lower than electrostatic and H-bonding.

Preliminary adsorption tests

The results from preliminary tests have indicated that the best conditions of adsorption experiment were as follows: smaller particle size (0.177 mm), stirring speed of 120 rpm and acidic media (pH = 2). The last process parameter has to be considered as a key parameter of the adsorption process. The dye uptake by CPS-AC rises with the decreasing of pH solution by achieving an approximately removal of 98% at pH = 2. In other words, as pH of dye solution decreased, more protons are available in the bulk liquid and the number of negatively charged active sites is reduced over the adsorbent surface [18]. This result agrees with the observed functional groups identified during the FTIR analysis, where in acidic media the carboxylic groups can turn positively charged by attracting the anionic sulfonate groups of the DYA dye molecule.

Kinetic tests

Results from the kinetic experiments of DYA dye adsorption process onto CPS-AC showed that a dye removal of 50% was reached within 9 hours. The equilibrium state was established after 40 hours of process time by achieving a dye uptake approximately $12 \text{ mg}\cdot\text{g}^{-1}$. The fit of experimental data by the kinetic models (pseudo-first, pseudo-second order and Elovich) are illustrated in Fig. 4, and the estimated parameters values are presented in Table 4.

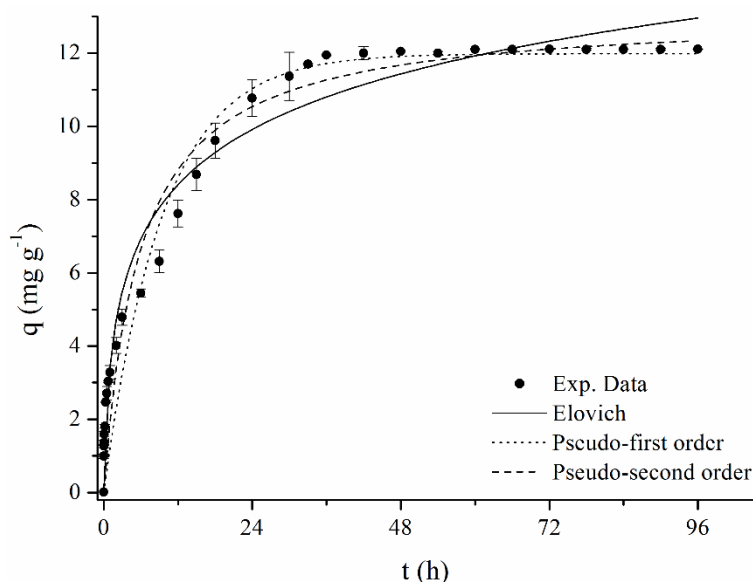


Fig. 4 Direct yellow ARLE dye adsorption kinetics by using CPS-AC (Experimental conditions: pH = 2.0, temperature 30 °C, stirring speed 120 rpm, particle size 0.177 mm and $C_0 = 70 \text{ mg}\cdot\text{L}^{-1}$)

Among the evaluated adsorption kinetic models, Elovich has shown best performance when fitted DYA dye adsorption kinetic data. The quantitative analysis of the fit by using Elovich model has shown that its correlation coefficient (r^2) was the highest one, which corresponded to the lowest values of objective function (F_{obj}) and reduced chi-square (χ^2), respectively (see Table 4).

By analyzing Fig. 4 one may conclude that the best graphical interpretation of the adsorption dynamics can be considered when applying the pseudo-first order kinetic model in contrast to the statistical evaluation (see Table 4). It must be noted, that the final evaluation of the models power has to be based on the interpretation of the model parameters values and especially

with the value of $q_{eq,model}$ and how the value of this parameter corresponds to the experimentally determined $q_{eq,exp}$.

Table 4. Estimated parameters values of adsorption kinetic models

Model	Parameters	Values
Pseudo-first order	$q_{eq} \text{ (mg} \cdot \text{g}^{-1}\text{)}$	11.98
	$k_1 \text{ (h}^{-1}\text{)}$	0.1053
	r^2	0.9443
	χ^2	1.2128
	F_{obj}	35.17
Pseudo-second order	$q_{eq} \text{ (mg} \cdot \text{g}^{-1}\text{)}$	13.08
	$k_2 \text{ (g} \cdot \text{mg}^{-1} \cdot \text{min}^{-1}\text{)}$	0.0132
	r^2	0.9581
	χ^2	0.9122
	F_{obj}	26.45
Elovich	$\alpha \text{ (mg} \cdot \text{g}^{-1} \cdot \text{h}^{-1}\text{)}$	8.096
	$\beta \text{ (g} \cdot \text{mg}^{-1}\text{)}$	0.4529
	r^2	0.9711
	χ^2	0.6301
	F_{obj}	18.27

The model proposed by Weber and Morris [75] was used in order to evaluate the hypothesis of intra-particle diffusion steps taking place in the adsorption process of DYA dye onto CPS-AC. A plot of dye uptake amount versus the square root of time is assumed to provide a linear relation (see Fig. 5), obtaining values of k_{dif} and C (see Table 5). As several diffusion steps were assumed to take place during the dye uptake, the plots of q vs $t^{1/2}$ were separated into several linear zones.

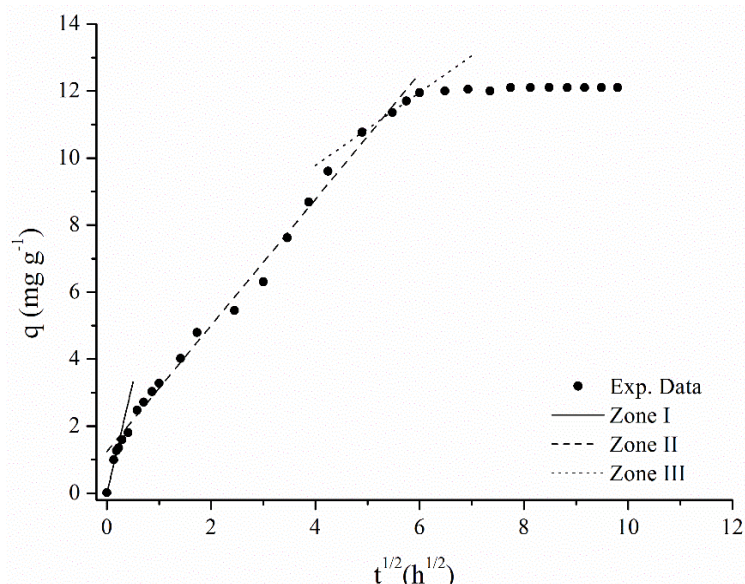


Fig. 5 Weber and Morris kinetic model

Table 5. Estimated parameters values of Weber and Morris kinetic models

Zone	Parameters	Values
I	$k_{dif,1} \text{ (mg} \cdot \text{g}^{-1} \cdot \text{h}^{-1/2}\text{)}$	6.631
	r^2	0.9664
II	$k_{dif,2} \text{ (mg} \cdot \text{g}^{-1} \cdot \text{h}^{-1/2}\text{)}$	1.880
	$C_2 \text{ (mg} \cdot \text{g}^{-1}\text{)}$	1.247
	r^2	0.9886
III	$k_{dif,3} \text{ (mg} \cdot \text{g}^{-1} \cdot \text{h}^{-1/2}\text{)}$	1.091
	$C_3 \text{ (mg} \cdot \text{g}^{-1}\text{)}$	5.414
	r^2	0.9975

Observing Fig. 5, it has to be noticed, that there are three well defined regions at low, intermediate and high $t^{1/2}$ ranges. The first zone (0 to 0.5 $\text{h}^{1/2}$) is attributed to external surface adsorption, where diffusion rate constants have the highest diffusion rate value and boundary layer diffusion effect is null ($C_1 = 0$). The second and more extensive zone (0.5 to 5.2 $\text{h}^{1/2}$), is attributed to macro-pore diffusion, which showed non null boundary layer diffusion and the diffusion rate was much lower than that in external diffusion. Finally, the third zone (5.2 up to 6.0 $\text{h}^{1/2}$) is assigned to the micro-pore diffusion, having the lowest diffusion rate and the highest boundary layer. Finally, after this step the rate of the process slowed down until equilibrium is attained. Hence, the DYA dye adsorption process onto CPS-AC can be described as being controlled by particle diffusion, wherein the internal diffusion controlled the overall process.

This result is in agreement with the textural properties of the CPS-AC (see Table 1), where the adsorbent presents high specific surface area and microporosity values. In this sense, besides the surface adsorption step, the overall process will depend on the diffusion of the dye molecule from the liquid phase into the porous structure of the AC (i.e. macropores and micropores). However, considering the elevated values of micropore surface area ($416 \text{ m}^2 \cdot \text{g}^{-1}$) and micropore volume ($0.32 \text{ cm}^3 \cdot \text{g}^{-1}$) of the CPS-AC, the micropores diffusion step (Zone III) is considerably short. This behavior can be explained by the large DYA dye dimensions ($d_{long} = 4.0 \text{ nm}$, $d_{front} = 1.1 \text{ nm}$ and $d_{lat} = 0.8 \text{ nm}$) at Fig. 2, when compared to the average pore diameter ($D_p = 1.2 \text{ nm}$) at Table 1. Therefore, the DYA dye molecule has steric difficulties to diffuse into the smaller pores and may not achieve most of the micropores, remaining mostly at the macro and mesopore structure of the AC. In this way, the DYA dye adsorption capacity by CPS-AC could be improved by augmenting the pore diameter, which could be probably done by changing the activation methods and conditions at this adsorbent also by replacing the AC precursor raw material.

Equilibrium tests

Equilibrium adsorption data of DYA dye onto CPS-AC and their fitting by using of Langmuir, Freundlich, Tóth, Sips and Khan isotherms are illustrated in Fig. 6. The estimated parameter values of these models are presented in Table 6.

Among evaluated adsorption isotherms, Sips was the one that presented best DYA dye adsorption equilibrium data, which is proved by the values of r^2 , χ^2 and F_{obj} . It has to be noticed, that Sips, Khan and Tóth isotherms performed very well and showed very similar profiles to the one of Langmuir model. In addition, the values of parameters n , n_T and n_k , considering all cases, are close to unity and this fact give us confidence to reduce these isotherms to the Langmuir isotherm representation. In this particular range of experimental

study, model profiles cannot be discriminated because the difference of their predictions is negligible (see Fig. 6). Hence, one may safely assume that active sites are energetically homogeneous and most likely monolayer adsorption take place on adsorbent surface [31]. Therefore, Langmuir model can be considered as best isotherm to represent the equilibrium adsorption data for the given range of experimental study. The estimated parameters values of the Langmuir model were in agreement with other works published in the area and were as follows: the maximum adsorption capacity $q_{max} = 101.56 \pm 4.79 \text{ mg}\cdot\text{g}^{-1}$ and affinity constant $b = 0.044 \pm 0.005 \text{ L}\cdot\text{mg}^{-1}$.

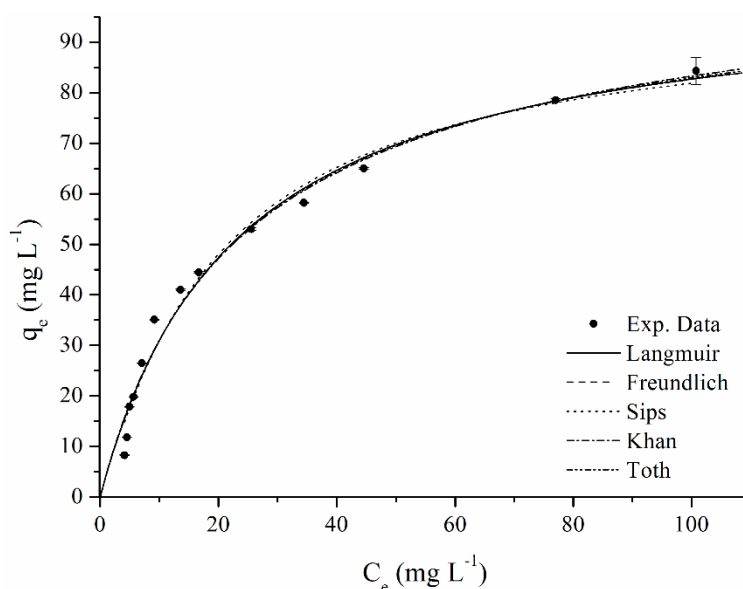


Fig. 6 Direct yellow ARLE dye adsorption equilibrium experimental data by using CPS-AC (Experimental conditions: pH = 2.0, temperature 30° C, stirring speed 120 rpm, particle size 0.177 mm and adsorption time of 48 h)

Therefore, the process involved the monolayer adsorption of DYA dye onto the active sites presented on the CPS-AC adsorbent surface, where the carboxylic groups acted as the main binding site attracting electrostatically the anionic sulfonate groups of the dye until its saturation at acidic pH values. In addition, hydrogen bonds may occur between the oxygen and nitrogen in the dye structure and the available hydrogen on the CPS-AC surface (e.g. hydroxyl, carboxyl groups). Finally, the hydrophobic interactions may take place, as well, among non-polar structures of the CPS-AC and aromatic rings in the DYA dye structure.

In spite of the fact that several molecular interactions may occurred during the adsorption process leading to an elevated affinity between the CPS-AC and the DYA dye, diffusional resistances at the micro-pores of the adsorbent were observed. This phenomenon reflected to a limitation of the adsorption capacity of the CPS-AC. Despite of the high removal rates of the DYA dye achieved by the used of CPS-AC, the sorption capacity still could be improved by increasing the adsorbent's pore size, focusing on a mesoporous material by other activation methods or by applying other biomass as a precursor of AC.

Table 6. Estimated parameters values of adsorption isotherms

Isotherm	Parameters	Values
Langmuir	q_{max} ($\text{mg}\cdot\text{g}^{-1}$)	101.56 ± 4.79
	b ($\text{L}\cdot\text{mg}^{-1}$)	0.044 ± 0.005
	r^2	0.9803
	χ^2	13.3514
	F_{obj}	146.8
Frendlich	k ($\text{mg}\cdot\text{g}^{-1}$)	10.45 ± 1.61
	n	0.468 ± 0.040
	r^2	0.9400
	χ^2	40.6902
	F_{obj}	447.6
Khan	q_{max} ($\text{mg}\cdot\text{g}^{-1}$)	89.39 ± 39.53
	b_k ($\text{L}\cdot\text{mg}^{-1}$)	0.051 ± 0.029
	n_k	0.941 ± 0.192
	r^2	0.9805
	F_{obj}	145.3
Sips	q_{max} ($\text{mg}\cdot\text{g}^{-1}$)	96.60 ± 9.23
	b_s ($\text{L}\cdot\text{mg}^{-1}$)	0.040 ± 0.009
	n	1.071 ± 0.140
	r^2	0.9809
	F_{obj}	143.4
Tóth	q_{max} ($\text{mg}\cdot\text{g}^{-1}$)	97.35 ± 32.40
	b_T ($\text{L}\cdot\text{mg}^{-1}$)	0.046 ± 0.017
	n_T	0.983 ± 0.125
	r^2	0.9804
	F_{obj}	146.5

Conclusion

The removal of direct yellow ARLE dye by coconut palm shell-based activated carbon was evaluated. Preliminary tests showed higher dye removal yields at stirring speed of 120 rpm, particle size of 0.177 mm and initial pH = 2. Under the best removal conditions, it was noticed a 40 hours equilibrium time and Elovich model was that one which best represented the dye adsorption kinetic data. The overall adsorption process was controlled by the particle diffusion inside the porous structure of the CPS-AC, wherein the macroporous diffusion was the most significant one. Microporous diffusion of the DYA-dye was limited due to steric limitations between the dye molecule size and the average pore size of the adsorbent. This fact was confirmed by the molecule structure dimension simulated by energy minimization molecular dynamics. Amongst all tested isotherms models, the monolayer adsorption behavior was observed as a main phenomenon; therefore, Langmuir isotherm represented adequately the dye adsorption equilibrium data by showing q_{max} of $101.56 \text{ mg}\cdot\text{g}^{-1}$ and b of $0.044 \text{ L}\cdot\text{mg}^{-1}$. By applying the functional groups characterization on the CPS-AC adsorbent was possible to identify the main adsorption sites and reactive groups of the DYA dye. Consequently, the intermolecular interactions responsible for adsorption process were recognized as electrostatic interactions, hydrogen bond and van der Waals forces. Based on the complex study and obtained kinetic and equilibrium results, we are confident that the application of the AC based on coconut palm shell is a challenging alternative and CPS-AC is a promising adsorbent for the removal of direct yellow ARLE dye. On the other hand,

complex technical-economical analysis of overall process should be performed in order to show the competitiveness of such application.

Acknowledgements

Authors thank to CAPES (Coordination for the Improvement of Higher Education Personnel), CNPq (National Counsel of Technological and Scientific Development) and Araucaria Foundation by financial support.

References

1. Ahmad R., R. Kumar (2010). Adsorptive removal of congo red dye from aqueous solution using bael shell carbon, *Applied Surface Science*, 257, 1628-1633.
2. Aksu Z. (2005). Application of biosorption for the removal of organic pollutants: A review, *Process Biochemistry*, 40, 997-1026.
3. Allen S. J., G. McKay, J. F. Porter (2004). Adsorption isotherm models for basic dye adsorption by peat in single and binary component systems, *Journal of Colloid and Interface Science*, 280, 322-333.
4. Amel K., M. A. Hassena, D. Kerroum (2012). Isotherm and kinetics study of biosorption of cationic dye onto banana peel, *Energy Procedia*, 19, 286-295.
5. Annadurai G., R. Juang, D. Lee (2002). Use of cellulose-based wastes for adsorption of dyes from aqueous solutions, *Journal of Hazardous Materials*, 92, 263-274.
6. Arica M. Y. G. Bayramoğlu (2007). Biosorption of reactive red-120 dye from aqueous solution by native and modified fungus biomass preparations of *lentinus sajor-caju*, *Journal of Hazardous Materials*, 149, 499-507.
7. Bekçi Z., Y. Seki, L. Cavas (2009). Removal of malachite green by using an invasive marine alga *caulerpa racemosa* var. *Cylindracea*, *Journal of Hazardous Materials*, 161, 1454-1460.
8. Blanchard G., M. Maunaye, G. Martin (1984). Removal of heavy metals from waters by means of natural zeolites, *Water Research*, 18, 1501-1507.
9. Colthup N. B. (1950). Spectra-structure correlations in the infra-red region, *Journal of the Optical Society of America*, 40, 397-400.
10. Daneshvar N., A. Oladegaragoze, N. Djafarzadeh (2006). Decolorization of basic dye solutions by electrocoagulation: An investigation of the effect of operational parameters, *Journal of Hazardous Materials*, 129, 116-122.
11. Djilani C., R. Zaghdoudi, A. Modarressi, M. Rogalski, F. Djazi, A. Lallam (2012). Elimination of organic micropollutants by adsorption on activated carbon prepared from agricultural waste, *Chemical Engineering Journal*, 189-190, 203-212.
12. El-Bindary A. A., A. Z. El-Sonbati, A. A. Al-Sarawy, K. S. Mohamed, M. A. Farid (2014). Adsorption and thermodynamic studies of hazardous azocoumarin dye from an aqueous solution onto low cost rice straw based carbons, *Journal of Molecular Liquids*, 199, 71-78.
13. El-Bindary A. A., A. Z. El-Sonbati, A. A. Al-Sarawy, K. S. Mohamed, M. A. Farid (2015). Removal of hazardous azopyrazole dye from an aqueous solution using rice straw as a waste adsorbent: Kinetic, equilibrium and thermodynamic studies, *Spectrochimica Acta Part A: Molecular and Biomolecular Spectroscopy*, 136, Part C, 1842-1849.
14. El Sikaily A., A. Khaled, A. E. Nemr, O. Abdelwahab (2006). Removal of methylene blue from aqueous solution by marine green alga *ulva lactuca*, *Chemistry and Ecology*, 22, 149-157.
15. Errais E., J. Duplay, M. Elhabiri, M. Khodja, R. Ocampo, R. Baltenweck-Guyot, F. Darragi (2012). Anionic rr120 dye adsorption onto raw clay: Surface properties and

- adsorption mechanism, *Colloids and Surfaces A: Physicochemical and Engineering Aspects*, 403, 69-78.
16. Espinoza-Quiñones F. R., A. N. Módenes, A. S. Câmara, G. Stutz, G. Tirao, S. M. Palácio, A. D. Kroumov, A. P. Oliveira, V. L. Alflen (2010). Application of high resolution X-ray emission spectroscopy on the study of Cr ion adsorption by activated carbon, *Applied Radiation and Isotopes*, 68, 2208-2213.
 17. Fernandez M. E., G. V. Nunell, P. R. Bonelli, A. L. Cukierman (2014). Activated carbon developed from orange peels: Batch and dynamic competitive adsorption of basic dyes, *Industrial Crops and Products*, 62, 437-445.
 18. Fiorentin L. D., D. E. G. Trigueros, A. N. Módenes, F. R. Espinoza-Quiñones, N. C. Pereira, S. T. D. Barros, O. A. A. Santos (2010). Biosorption of reactive blue 5g dye onto drying orange bagasse in batch system: Kinetic and equilibrium modeling, *Chemical Engineering Journal*, 163, 68-77.
 19. Freundlich H. M. F. (1906). Über die adsorption in lösungen, *Zeitschrift für Physikalische Chemie*, 57(A), 385-470.
 20. Furlan F. R., L. G. de Melo da Silva, A. F. Morgado, A. A. U. de Souza, S. M. A. Guelli Ulson de Souza (2010). Removal of reactive dyes from aqueous solutions using combined coagulation/flocculation and adsorption on activated carbon, *Resources, Conservation and Recycling*, 54, 283-290.
 21. Ghaedi M., B. Sadeghian, A. A. Pebdani, R. Sahraei, A. Daneshfar, C. Duran (2012). Kinetics, thermodynamics and equilibrium evaluation of direct yellow 12 removal by adsorption onto silver nanoparticles loaded activated carbon, *Chemical Engineering Journal*, 187, 133-141.
 22. Gil A., F. C. C. Assis, S. Albeniz, S. A. Korili (2011). Removal of dyes from wastewaters by adsorption on pillared clays, *Chemical Engineering Journal*, 168, 1032-1040.
 23. Gong R., Y. Jin, J. Sun, K. Zhong (2008). Preparation and utilization of rice straw bearing carboxyl groups for removal of basic dyes from aqueous solution, *Dyes and Pigments*, 76, 519-524.
 24. Grunewald G. C., R. S. Drago (1991). Carbon molecular sieves as catalysts and catalyst supports, *Journal of the American Chemical Society*, 113, 1636-1639.
 25. Guaratini C. C. I., M. V. B. Zanoni (2000). Corantes têxteis, *Química Nova*, 23, 71-78.
 26. Gusmão K. A. G., L. V. A. Gurgel, T. M. S. Melo, L. F. Gil (2013). Adsorption studies of methylene blue and gentian violet on sugarcane bagasse modified with edta dianhydride (edtad) in aqueous solutions: Kinetic and equilibrium aspects, *Journal of Environmental Management*, 118, 135-143.
 27. Halgren T. A. (1996). Merck molecular force field. I. Basis, form, scope, parameterization, and performance of MMFF94, *Journal of Computational Chemistry*, 17, 490-519.
 28. Hameed B. H., M. I. El-Khaiary (2008). Kinetics and equilibrium studies of malachite green adsorption on rice straw-derived char, *Journal of Hazardous Materials*, 153, 701-708.
 29. Huang X., X. Bo, Y. Zhao, B. Gao, Y. Wang, S. Sun, Q. Yue, Q. Li (2014). Effects of compound bioflocculant on coagulation performance and floc properties for dye removal, *Bioresource Technology*, 165, 116-121.
 30. Iqbal M. J., M. N. Ashiq (2007). Adsorption of dyes from aqueous solutions on activated charcoal, *Journal of Hazardous Materials*, 139, 57-66.
 31. Jeppu G. P., T. P. Clement (2012). A modified Langmuir-Freundlich isotherm model for simulating pH-dependent adsorption effects, *Journal of Contaminant Hydrology*, 129-130, 46-53.

32. Khan A. R., R. Atallah, A. AlHaddad (1997). Equilibrium adsorption studies of some aromatic pollutants from dilute aqueous solutions on activated carbon at different temperatures, *Journal of Colloid and Interface Science*, 194, 154-165.
33. Khanna A., V. K. Shetty (2014). Solar light induced photocatalytic degradation of Reactive Blue 220 (RB-220) dye with highly efficient Ag@TiO₂ core-shell nanoparticles: A comparison with UV photocatalysis, *Solar Energy*, 99, 67-76.
34. Khayet M., A. Y. Zahrim, N. Hilal (2011). Modelling and optimization of coagulation of highly concentrated industrial grade leather dye by response surface methodology, *Chemical Engineering Journal*, 167, 77-83.
35. Kiernan J. A. (2001). Classification and naming of dyes, stains and fluorochromes, *Biotechnic & Histochemistry*, 76, 261-278.
36. Kismir Y., A. Z. Aroguz (2011). Adsorption characteristics of the hazardous dye brilliant green on saklıkent mud, *Chemical Engineering Journal*, 172, 199-206.
37. Konicki W., D. Sibera, E. Mijowska, Z. Lendzion-Bieluń, U. Narkiewicz (2013). Equilibrium and kinetic studies on acid dye Acid Red 88 adsorption by magnetic ZnFe₂O₄ spinel ferrite nanoparticles, *Journal of Colloid and Interface Science*, 398, 152-160.
38. Lagergren S. (1898). About the theory of so-called adsorption of soluble substances, *Kungliga Svenska Vetenskapsakademiens Handlingar*, 24, 1-39.
39. Langmuir I. (1916). The constitution and fundamental properties of solids and liquids. Part i. Solids, *Journal of the American Chemical Society*, 38, 2221-2295.
40. Lau Y.-Y., Y.-S. Wong, T.-T. Teng, N. Morad, M. Rafatullah, S.-A. Ong (2014). Coagulation-flocculation of azo dye acid orange 7 with green refined laterite soil, *Chemical Engineering Journal*, 246, 383-390.
41. Leyva-Ramos R. (1989). Effect of temperature and pH on the adsorption of an anionic detergent on activated carbon, *Journal of Chemical Technology & Biotechnology*, 45, 231-240.
42. Li X.-Z., K.-L. Wu, C. Dong, S.-H. Xia, Y. Ye, X.-W. Wei (2014). Size-controlled synthesis of Ag₃PO₄ nanorods and their high-performance photocatalysis for dye degradation under visible-light irradiation, *Materials Letters*, 130, 97-100.
43. Liang C.-Z., S.-P. Sun, F.-Y. Li, Y.-K. Ong, T.-S. Chung (2014). Treatment of highly concentrated wastewater containing multiple synthetic dyes by a combined process of coagulation/flocculation and nanofiltration, *Journal of Membrane Science*, 469, 306-315.
44. Liberatti V. R., R. Afonso, A. C. Lucilha, P. R. Catarini da Silva, L. H. Dall'Antonia (2014). Fotocatálise do azul de metileno na presença de óxido de bismuto sob irradiação de luz uv e solar, *Semina: Ciências Exatas e Tecnológicas*, 35, 55-55.
45. Limousin G., J. P. Gaudet, L. Charlet, S. Szenknect, V. Barthès, M. Krimissa (2007). Sorption isotherms: A review on physical bases, modeling and measurement, *Applied Geochemistry*, 22, 249-275.
46. Low M. J. D. (1960). Kinetics of chemisorption of gases on solids, *Chem Rev*, 60, 267-312.
47. Mahmoodi N. M., R. Salehi, M. Arami (2011). Binary system dye removal from colored textile wastewater using activated carbon: Kinetic and isotherm studies, *Desalination*, 272, 187-195.
48. Manenti D., P. Soares, T. C. V. Silva, A. Módenes, F. Espinoza-Quñones, R. Bergamasco, R. R. Boaventura, V. P. Vilar (2015). Performance evaluation of different solar advanced oxidation processes applied to the treatment of a real textile dyeing wastewater, *Environmental Science and Pollution Research*, 22, 833-845.
49. Manenti D. R., F. H. Borba, A. N. Módenes, F. R. Espinoza-Quñones, S. M. Palácio, V. J. P. Vilar, R. Bergamasco (2014). Avaliação do desempenho de um sistema de

- tratamento utilizando os processos eletrocoagulação e foto-fenton integrados no tratamento de um efluente têxtil, *Engevista*, 16, 420-431.
50. Manenti D. R., A. N. Módenes, P. A. Soares, F. R. Espinoza-Quiñones, R. A. R. Boaventura, R. Bergamasco, V. J. P. Vilar (2014). Assessment of a multistage system based on electrocoagulation, solar photo-fenton and biological oxidation processes for real textile wastewater treatment, *Chemical Engineering Journal*, 252, 120-130.
 51. Manenti D. R., P. A. Soares, A. N. Módenes, F. R. Espinoza-Quiñones, R. A. R. Boaventura, R. Bergamasco, V. J. P. Vilar (2015). Insights into solar photo-fenton process using iron(III)-organic ligand complexes applied to real textile wastewater treatment, *Chemical Engineering Journal*, 266, 203-212.
 52. Módenes A. N., A. A. Ross, B. V. Souza, J. Dotto, C. Q. Geraldi, F. R. Espinoza-quiñones, A. D. Kroumov (2013). Biosorption of BF-4B reactive red dye by using leaves of macrophytes *Eichhornia crassipes*, *International Journal Bioautomation*, 17, 33-44.
 53. Módenes A. N., F. B. Scheufele, C. J. Glitz Jr., A. Colombo, F. R. Espinoza-Quiñones, A. D. Kroumov (2014). Kinetics and equilibrium study of black krom KJR dye sorption by bone-based activated carbon, *International Journal Bioautomation*, 18, 251-264.
 54. Morshedi D., Z. Mohammadi, M. M. Akbar Boojar, F. Aliakbari (2013). Using protein nanofibrils to remove azo dyes from aqueous solution by the coagulation process, *Colloids and Surfaces B: Biointerfaces*, 112, 245-254.
 55. Moubarak F., R. Atmani, I. Maghri, M. Elkouali, M. Talbi, M. L. Bouamrani, M. Salouhi, A. Kenz (2014). Elimination of methylene blue dye with natural adsorbent “banana peels powder”, *Global Journal of Science Frontier Research: B Chemistry*, 14(1), 39-44.
 56. Movasaghi Z., S. Rehman, D.I. ur Rehman (2008). Fourier transform infrared (FTIR) spectroscopy of biological tissues, *Applied Spectroscopy Reviews*, 43, 134-179.
 57. Ncibi M. C., A. M. B. Hamissa, A. Fathallah, M. H. Kortas, T. Baklouti, B. Mahjoub, M. Seffen (2009). Biosorptive uptake of methylene blue using mediterranean green alga *Enteromorpha* spp, *Journal of Hazardous Materials*, 170, 1050-1055.
 58. Noreen S., H. N. Bhatti (2014). Fitting of equilibrium and kinetic data for the removal of novacron orange p-2r by sugarcane bagasse, *Journal of Industrial and Engineering Chemistry*, 20, 1684-1692.
 59. Öztürk A., E. Malkoc (2014). Adsorptive potential of cationic basic yellow 2 (BY2) dye onto natural untreated clay (NUC) from aqueous phase: Mass transfer analysis, kinetic and equilibrium profile, *Applied Surface Science*, 299, 105-115.
 60. Palácio S. M., F. R. Espinoza-Quiñones, A. N. Módenes, D. R. Manenti, C. C. Oliveira, J. C. Garcia (2012). Optimised photocatalytic degradation of a mixture of azo dyes using a $\text{TiO}_2/\text{H}_2\text{O}_2/\text{UV}$ process, *Water Science and Technology*, 65, 1392-1398.
 61. Pendleton P., S. H. Wu (2003). Kinetics of dodecanoic acid adsorption from caustic solution by activated carbon, *Journal of Colloid and Interface Science*, 266, 245-250.
 62. Purnomo C. W., C. Salim, H. Hinode (2011). Preparation and characterization of activated carbon from bagasse fly ash, *Journal of Analytical and Applied Pyrolysis*, 91, 257-262.
 63. Robinson T., B. Chandran, P. Nigam (2002). Removal of dyes from a synthetic textile dye effluent by biosorption on apple pomace and wheat straw, *Water Research*, 36, 2824-2830.
 64. Satapathy M. K., P. Das (2014). Optimization of crystal violet dye removal using novel soil-silver nanocomposite as nanoadsorbent using response surface methodology, *Journal of Environmental Chemical Engineering*, 2, 708-714.
 65. Shi B., G. Li, D. Wang, C. Feng, H. Tang (2007). Removal of direct dyes by coagulation: The performance of preformed polymeric aluminum species, *Journal of Hazardous Materials*, 143, 567-574.

66. Sidiras D., F. Batzias, E. Schroeder, R. Ranjan, M. Tsapatsis (2011). Dye adsorption on autohydrolyzed pine sawdust in batch and fixed-bed systems, *Chemical Engineering Journal*, 171, 883-896.
67. Sips R. (1948). On the structure of a catalyst surface, *Journal of Chemical Physics*, 16, 490-495.
68. Smidt E., K. Meissl (2007). The applicability of fourier transform infrared (FT-IR) spectroscopy in waste management, *Waste Management*, 27, 268-276.
69. Szyguła A., E. Guibal, M. A. Palacín, M. Ruiz, A. M. Sastre (2009). Removal of an anionic dye (acid blue 92) by coagulation-flocculation using chitosan, *Journal of Environmental Management*, 90, 2979-2986.
70. Timur S., I. C. Kantarli, S. Onenc, J. Yanik (2010). Characterization and application of activated carbon produced from oak cups pulp, *Journal of Analytical and Applied Pyrolysis*, 89, 129-136.
71. Tóth J. (1971). State equations of the solid-gas interface layers, *Acta Chimica Academiae Scientiarum Hungaricae*, 69, 311-317.
72. Tsai W. T., C. Y. Chang, M. C. Lin, S. F. Chien, H. F. Sun, M. F. Hsieh (2001). Adsorption of acid dye onto activated carbons prepared from agricultural waste bagasse by $ZnCl_2$ activation, *Chemosphere*, 45, 51-58.
73. Vasanth Kumar K., S. Sivanesan (2006). Equilibrium data, isotherm parameters and process design for partial and complete isotherm of methylene blue onto activated carbon, *Journal of Hazardous Materials*, 134, 237-244.
74. Wang M.-X., Q.-L. Zhang, S.-J. Yao (2015). A novel biosorbent formed of marine-derived penicillium janthinellum mycelial pellets for removing dyes from dye-containing wastewater, *Chemical Engineering Journal*, 259, 837-844.
75. Weber W. J., J. C. Morris (1963). Kinetics of adsorption on carbon from solution, *Journal of the Sanitary Engineering Division*, 89, 31-60.
76. Xu X., B.-Y. Gao, Q.-Y. Yue, Q.-Q. Zhong (2010). Preparation and utilization of wheat straw bearing amine groups for the sorption of acid and reactive dyes from aqueous solutions, *Journal of Hazardous Materials*, 182, 1-9.
77. Zhang C., L. Gu, Y. Lin, Y. Wang, D. Fu, Z. Gu (2009). Degradation of X-3B dye by immobilized TiO_2 photocatalysis coupling anodic oxidation on BDD electrode, *Journal of Photochemistry and Photobiology A: Chemistry*, 207, 66-72.
78. Zhang R., J. Zhang, X. Zhang, C. Dou, R. Han (2014). Adsorption of congo red from aqueous solutions using cationic surfactant modified wheat straw in batch mode: Kinetic and equilibrium study, *Journal of the Taiwan Institute of Chemical Engineers*, 45, 2578-2583.
79. Zhang X. D., J. D. Hao, W. S. Li, H. J. Jin, J. Yang, Q. M. Huang, D. S. Lu, H. K. Xu (2009). Synergistic effect in treatment of C.I. Acid Red 2 by electrocoagulation and electrooxidation, *Journal of Hazardous Materials*, 170, 883-887.
80. Zhang Z., I. M. O'Hara, G. A. Kent, W. O. S. Doherty (2013). Comparative study on adsorption of two cationic dyes by milled sugarcane bagasse, *Industrial Crops and Products*, 42, 41-49.
81. Zhao B., Y. Shang, W. Xiao, C. Dou, R. Han (2014). Adsorption of congo red from solution using cationic surfactant modified wheat straw in column model, *Journal of Environmental Chemical Engineering*, 2, 40-45.

Prof. Aparecido Nivaldo Módenes, Ph.D.E-mail: anmodenes@yahoo.com.br

Prof. Módenes graduated and obtained his Ph.D. in Chemical Engineering. He is a Professor at West Parana State University and a head of Process Development and Biotechnology Center. Prof. Módenes' scientific interests are in separation processes, wastewater purification, modelling and chemical processes optimization.

Fabiano Bisinella Scheufele, Ph.D.E-mail: fabianoscheufele@gmail.com

Fabiano Scheufele graduated in Chemical Engineering from West Parana State University and recently defended his Ph.D. thesis in State University of Maringá. His current interests are in separation processes, particulate systems, wastewater treatment, and adsorption processes.

Prof. Fernando Rodolfo Espinoza-Quiñones, Ph.D.E-mail: f.espinoza@terra.com.br

Prof. Espinoza-Quiñones graduated and obtained his Ph.D. in the field of Nuclear Physics. He is a Professor at West Parana State University and a head of postgraduate program in Chemical Engineering. Prof. Espinoza-Quiñones' current interests are in material science with application of different advanced methods of analysis and in wastewater treatment from heavy metals by using plants and electrocoagulation techniques.

Patrícia Simões Carraro de Souza, M.Sc. StudentE-mail: patricia.carraro@hotmail.com

Patrícia de Souza graduated in Chemistry, and currently studying for M.Sc. in the field of Chemical Engineering at West Parana State University. Her scientific interests are in advanced oxidation processes and adsorption.

Camila Raquel Betin Cripa, M.Sc. StudentE-mail: camilacripa@gmail.com

Camila Cripa graduated and currently studying for M.Sc. in the field of Chemical Engineering at West Parana State University. Her scientific interests are in advanced oxidation processes and adsorption.

Joelmir dos Santos, M.Sc. StudentE-mail: joe.dossantos@hotmail.com

Joelmir dos Santos graduated in Chemical Process Technology from the Federal Technological University of Paraná. Currently he is studying for M.Sc. in Chemical Engineering at West Parana State University. His scientific interests are in environmental monitoring and adsorption.

Assoc. Prof. Vilmar Steffen, Ph.D.E-mail: eq.vilmar@hotmail.com

Vilmar Steffen graduated in Chemical Engineering from the State University of Western Paraná (2007), M.Sc. degree in Chemical Engineering from the State University of Western Paraná (2010) and a Ph.D. in Chemical Engineering from the State University of Maringa (2014). Assoc. Prof. Steffen has an experience in modeling and simulation, with emphasis on reactive distillation, adsorption and Poisson-Boltzmann equation. Currently he is an Associate Professor at Federal Technological University of Paraná.

Alexander Dimitrov Kroumov, Ph.D.E-mail: adkrumov@microbio.bas.bg, adkrumov@gmail.com

Alexander Kroumov obtained his Ph.D. in the field of Technical Sciences (1987) from D. I. Mendeleev Institute of Chemical Technology, Moscow, Russia, Department of Cybernetics of Chemical-Technology Processes, with a Ph.D. thesis titled "Development of mathematical models and software for scale-up of tower bioreactors". Alexander Kroumov obtained B.Sc. and M.Sc. degrees in Chemical Engineering (1979) from the Institute of Chemical Engineering, Sofia, Bulgaria. His scientific interests are in the field of green technologies, bioprocess development and bioreactors/photobioreactors design.